Sains Malaysiana 54(9)(2025): 2211-2226
http://doi.org/10.17576/jsm-2025-5409-09

Synthesis and Characterization of Fe_3O_4/rGO/Ag Composites for Electrocatalytic Oxygen Reduction Reaction (ORR)

(Sintesis dan Pencirian Komposit Fe_3O_4/rGO/Ag untuk Tindak Balas Pengurangan Oksigen Elektrokatalitik (ORR))

KOMATY MARAN[1], SARAH ILYANIE ROSWADI[1], MOHD AFIFI JUSOH[2] & FARHANINI YUSOFF[1,*]

[1]*Faculty of Science and Marine Environment, Universiti Malaysia Terengganu, 21030 Kuala Terengganu, Terengganu, Malaysia*
[2]*Faculty of Ocean Engineering Technology, Universiti Malaysia Terengganu, 21030 Kuala Terengganu, Terengganu, Malaysia*

Received: 11 September 2024/Accepted: 18 July 2025

ABSTRACT

The oxygen reduction reaction (ORR) plays a pivotal role in fuel cells, making the discovery of efficient and cost-effective catalysts to substitute platinum crucial for the progress of sustainable energy technologies. This study investigates a new rGO/Fe_3O_4/Ag composite as a potential low-cost substitute for platinum-based cathode materials in ORR applications due to platinum's drawbacks. Reduced graphene oxide incorporated with iron (III) oxide and silver nanoparticles were synthesized through a modified one-pot process, denoted as rGO/Fe_3O_4/Ag. This study is the first to utilize rGO/Fe_3O_4/Ag as an ORR catalyst. Synthesis began with the formation of graphene oxide, followed by its reduction, the addition of Fe^{2+} and Fe^{3+}, and the introduction of silver nanoparticles via silver nitrate ($AgNO_3$) to produce the novel electrocatalyst. Physicochemical and electrochemical characterization was performed using Fourier transform infrared (FTIR) spectroscopy, X-ray diffraction (XRD), scanning electron microscopy-energy dispersive X-ray (SEM-EDX), Brunauer-Emmett-Teller (BET) analysis, and cyclic voltammetry (CV). FTIR confirmed the presence of functional groups such as O-H, C=C, C=O, C-O, C-Fe, and C-Ag in the nanocomposites. XRD identified average crystalline sizes, with diffraction peaks confirming the formation of rGO/Fe_3O_4/Ag. SEM-EDX analysis showed well-dispersed Fe_3O_4 and Ag nanoparticles on rGO sheets, and BET analysis indicated the nanocomposites were mesoporous, with a surface area of 81.60 m^2/g for rGO/Fe_3O_4/Ag. Electrochemical characterization showed that the modified rGO/Fe_3O_4/Ag exhibited significant redox responses, indicating enhanced electrochemical activity compared to the bare GCE. In the ORR analysis, the rGO/Fe_3O_4/Ag demonstrated a positive shift in the cyclic voltammogram, suggesting improved current density and superior ORR performance relative to the bare GCE. These results strongly suggest that rGO/Fe_3O_4/Ag can be an effective replacement for platinum in ORR applications as a cathode material.

Keywords: Cyclic voltammetry; electrocatalyst; graphene; iron oxide; oxygen reduction reaction (ORR)

ABSTRAK

Tindak balas pengurangan oksigen (ORR) memainkan peranan penting dalam sel bahan api, menjadikan penemuan pemangkin yang cekap dan kos efektif untuk menggantikan platinum penting untuk kemajuan teknologi tenaga mampan. Penyelidikan ini mengkaji komposit rGO/ Fe_3O_4/Ag baharu sebagai pengganti kos rendah yang berpotensi untuk bahan katod berasaskan platinum dalam aplikasi ORR disebabkan oleh kelemahan platinum. Grafena oksida terkurang yang digabungkan dengan oksida besi (III) dan nanozarah perak telah disintesis melalui proses satu periuk yang diubah suai, dilambangkan sebagai rGO/Fe_3O_4/Ag. Penyelidikan ini merupakan kajian pertama yang menggunakan rGO/Fe_3O_4/Ag sebagai katalis ORR. Sintesis bermula dengan pembentukan grafin oksida, diikuti oleh penurunannya, penambahan Fe^{2+} dan Fe^{3+} dan pengenalan nanozarah perak melalui nitrat perak ($AgNO_3$) untuk menghasilkan elektrokatalis baru. Pencirian fizikal-kimia dan elektrokimia dilakukan dengan menggunakan spektroskopi transformasi Fourier inframerah (FTIR), pembelauan sinar-X (XRD), mikroskop elektron pengesan-tenaga-sebaran X-ray (SEM-EDX), analisis Brunauer-Emmett-Teller (BET) dan voltametri berkitar (CV). FTIR mengesahkan kehadiran kumpulan berfungsi seperti O-H, C=C, C = O, C-O, C-Fe dan C-Ag dalam nanokomposit. XRD mengenal pasti saiz kristal purata dengan puncak difraksi mengesahkan pembentukan rGO/Fe_3O_4/Ag. Analisis SEM-EDX mendedahkan nanozarah Fe_3O_4 dan Ag yang tersebar dengan baik pada permukaan rGO dan analisis BET menunjukkan nanokomposit adalah 'mesoporous' dengan kawasan permukaan 81.60 m^2/g untuk rGO/Fe_3O_4/Ag. Pencirian elektrokimia menunjukkan bahawa rGO/Fe_3O_4/Ag yang diubah suai menunjukkan respons redoks yang signifikan; peningkatan aktiviti elektrokimia berbanding dengan GCE. Dalam analisis ORR, rGO/ Fe_3O_4/Ag menunjukkan pergeseran positif dalam voltamogram kitaran yang menunjukkan peningkatan kepadatan arus

dan prestasi ORR yang lebih baik berbanding GCE sahaja. Hasil ini menunjukkan bahawa rGO/Fe_3O_4/Ag boleh menjadi pengganti platinum yang berkesan dalam aplikasi ORR sebagai bahan katod.

Kata kunci: Grafin; katalis; oksida besi; tindak balas pengurangan oksigen (ORR); voltametri berkitar

INTRODUCTION

Renewable energy, often referred to as clean energy has garnered significant interest in recent years due to its continuous replenishment and benefits for the environment. Malaysia, like many other countries is progressively increasing its use of renewable energy sources. This transition is not only essential for environmental sustainability but also economically advantageous. Based on the findings of the International Renewable Energy Agency (2023), Malaysia has the potential to save an estimated amount of USD 9 billion to USD 13 billion per year by 2050 by implementing renewable energy sources. This cost reduction would be achieved by minimising costs related to energy, climate, and health (*Renewables Are the Solution to Malaysia's Sustainable Future and Renewed Climate Ambition* 2023). Thus, the increased use of renewable energy holds promise for multifaceted benefits.

Among the various renewable energy technologies being explored, fuel cells have emerged as a particularly promising solution. As the demand for sustainable energy continues to rise, the focus has intensified on technologies that are not only clean but also efficient and scalable. Fuel cells fit these criteria well, being one of the most potential and cost-effective renewable energy technologies due to their exceptional energy conversion efficiency (Khan et al. 2019). Unlike conventional combustion-based systems, fuel cells convert chemical energy directly into electrical energy through electrochemical reactions, making them a highly recommended green technology (Mohammed et al. 2019). Central to their operation is Oxygen Reduction Reaction (ORR), a critical electrochemical process that plays a vital role in improving fuel cell performance. It is an electrochemical process where oxygen molecules are reduced to water or hydrogen peroxide. The four-electron reduction pathway to water is particularly favorable in fuel cells due to higher current outputs (Peng & Wei 2020). Despite its benefits, ORR is characterized by sluggish kinetics, necessitating the use of catalysts to accelerate the reaction and enhance fuel cell performance (He et al. 2020).

Despite the progress in developing ORR catalysts, there remain significant challenges. Platinum-based catalysts, although effective, are expensive and scarce, limiting their widespread application (Shao et al. 2018). The high cost and limited availability of platinum necessitate the search for alternative catalysts that are both cost-effective and efficient. Non-precious metal catalysts, including iron-based materials, have shown promise but often suffer from issues such as stability, activity, and durability (Kumar et al. 2018). Moreover, the scalability of these catalysts for commercial applications remains a significant hurdle. Numerous catalysts have encountered significant obstacles in scaling for commercial ORR applications, chiefly due to concerns regarding cost, stability, and practical performance. Platinum-based catalysts, such as Pt/C, provide exceptional catalytic efficiency but are constrained by high costs, scarcity, and degradation mechanisms, including nanoparticle agglomeration, dissolution, and CO poisoning during extended operation (Shao, Yin & Gao 2007). Iron–nitrogen–carbon (Fe–N–C) catalysts offer a promising non-precious alternative; however, their practical application is frequently impeded by instability in acidic conditions and oxidative degradation of active sites, especially due to hydrogen peroxide generation during the oxygen reduction reaction (ORR) (Gu et al. 2023). Alternative candidates such as MnO_2 and Co_3O_4 exhibit low conductivity and inadequate durability, respectively (Cui et al. 2020). While silver-based catalysts demonstrate satisfactory performance in alkaline environments, they display diminished activity and restricted stability in acidic conditions, limiting their wider applicability. These examples illustrate the challenge of attaining equilibrium among activity, durability, and scalability in ORR catalysts, emphasizing the necessity for novel materials that offer enhanced long-term performance and cost-efficiency. Therefore, there is an urgent need to develop new catalyst materials that can provide high catalytic performance, stability, and cost-effectiveness for ORR in fuel cells.

Extensive research has been conducted on graphene-based materials as prospective electrocatalysts for oxygen reduction reaction (ORR) because of their distinctive characteristics. Graphene is a monolayer of carbon atoms structured in a two-dimensional hexagonal pattern, created by sp^2 hybridization (Chandrasekaran et al. 2020; Cui et al. 2022). Since its discovery in 2004, graphene has been hailed as a ground-breaking material in science and technology, leading to a Nobel Prize in Physics in 2010. Its widespread interest is driven by its multifunctional properties, including excellent electrical conductivity, extensive surface area, and robust mechanical strength (Goyal et al. 2022). However, the practical application of graphene is often limited by the challenges in synthesizing defect-free graphene on a large scale. This issue is typically addressed by using reduced graphene oxide (rGO), a derivative of graphene that retains many of its desirable properties while being more accessible to synthesize (Smith et al. 2019; Tarcan et al. 2020). rGO exists in a state between graphene and graphene oxide (GO), offering a balance between electrical conductivity and ease of production.

Iron, the most abundant metal on Earth, plays a significant role in various biochemical processes and is available in multiple crystalline forms, including hematite (Fe_2O_3), magnetite (Fe_3O_4), and wustite (FeO) (Ajinkya et al. 2020). Magnetite (Fe_3O_4) has gained attention due to its high surface area, paramagnetic properties, and substantial iron content (78%) (Ganapathe et al. 2020). Combining magnetite with rGO can enhance the catalytic activity in ORR by leveraging the magnetic properties of Fe_3O_4 and the conductive network of rGO. This combination promises increased surface area, lower toxicity, and enhanced electrochemical conductivity (Yusoff, Suresh & Khairul 2022). Silver nanoparticles (AgNPs) are another component incorporated into the hybrid material due to their unique catalytic properties. AgNPs can form thin films on various substrates, which are highly effective in catalysis, electrochemical methods, thermal decomposition, and microwave irradiation processes (Sharma et al. 2021). Incorporating AgNPs into the Fe_3O_4/rGO composite is expected to further improve electron transfer rates, enhance electrochemical stability, and increase electrocatalytic efficiency and biocompatibility (Iriarte-Mesa et al. 2020; Sharma et al. 2021).

Recent studies have demonstrated the potential of various metal and carbon-based nanocomposites in enhancing ORR activity. For instance, an investigation conducted by Zhao et al. (2021) shown that Fe-N-C catalysts demonstrated exceptional ORR performance due to the synergistic effects of iron and nitrogen doping in the carbon framework. Similarly, Sharma et al. (2021) reported that Ag-decorated rGO composites significantly improved ORR activity, highlighting the role of silver in enhancing catalytic properties. Furthermore, He et al. (2021) demonstrated that Fe_3O_4 nanoparticles supported on rGO resulted in improved activity and stabilisation for ORR, due to the synergistic effects of Fe_3O_4 and rGO.

Graphene and its derivatives have shown immense potential as ORR catalysts owing to its distinctive properties, including a large surface area, exceptional electrical conductivity, and mechanical robustness. Recent advancements in the synthesis and modification of graphene-based materials have opened new avenues for developing efficient and cost-effective ORR catalysts. For example, nitrogen-doped graphene has been shown to significantly enhance ORR activity due to the introduction of active sites for oxygen adsorption and reduction (Singh, Takeyasu & Nakamura 2019). Furthermore, there has been significant research conducted on transition metal oxides, such as Fe_3O_4, because of their remarkable stability and catalytic activity as a possible catalyst for the oxygen reduction reaction (ORR) (He et al. 2021; Song et al. 2022).

Incorporating Ag nanoparticles into graphene-based materials has also been shown to enhance ORR activity. Ag nanoparticles provide additional active sites for oxygen adsorption and reduction, thereby improving the overall catalytic performance. A study by Chen et al. (2021) demonstrated that Ag-decorated rGO exhibited excellent ORR activity, attributed to the synergistic effects of Ag and rGO. Furthermore, the combination of Fe_3O_4 and Ag nanoparticles with rGO has shown promising results in enhancing ORR activity. A study by Idris et al. (2018) reported that Fe_3O_4/Ag/rGO composites exhibited superior ORR activity and stability compared to individual components, highlighting the importance of synergistic effects in enhancing catalytic performance.

In this study, the aim was to synthesize rGO combined with iron oxide and silver nanoparticles and investigate their physical, chemical, and electrochemical properties, particularly their efficiency as catalysts in ORR applications. The synthesis process begins with producing GO from pure graphite using the modified Hummer's method, followed by the reduction of GO to rGO using strong reducing agents. Subsequently, rGO is combined with iron oxide, and finally, silver nanoparticles are incorporated to produce the hybrid material. The hypothesis is that adding silver to the metal-graphene composite will enhance electrochemical stability, electrocatalytic efficiency, resistance, and electron transfer rates. The expected outcome is improved physical, chemical, and electrochemical properties of the hybrid material, making it a viable candidate for ORR applications.

MATERIALS AND METHODS

Chemicals and Reagents

Graphite powder (analytical grade, Sigma-Aldrich, USA), sodium nitrate ($NaNO_3$, reagent grade, Sigma-Aldrich, USA), sulfuric acid (H_2SO_4, 98%, Sigma-Aldrich, USA), and potassium permanganate ($KMnO_4$, reagent grade, Sigma-Aldrich, USA) were used to synthesize graphene oxide (GO). Ferrous chloride tetrahydrate ($FeCl_2.4H_2O$, Sigma-Aldrich, USA) and ferric chloride hexahydrate ($FeCl_3.6H_2O$, Sigma Aldrich, USA) were used in producing magnetite nanoparticles. Sodium hydroxide (NaOH, analytical grade, Sigma-Aldrich) was used for synthesizing purposes and both hydrazine hydrate ($N_2H_4{\cdot}H_2O$, 80%, Sigma-Aldrich) and sodium borohydride ($NaBH_4$, reagent grade, ≥98%, Sigma-Aldrich) were used in this experiment too for reducing purposes. Besides that, in order to perform silver nanoparticles, silver nitrate ($AgNO_3$) was used in this experiment. Potassium hydroxide (KOH, pellets, ≥85%, Sigma-Aldrich) was used as an electrolyte in ORR analysis. Potassium ferrocyanide ($K_4[Fe(CN)_6]$, trihydrate, reagent grade, Sigma-Aldrich) and potassium chloride (KCl, ≥99%, Sigma-Aldrich) was used in the electrolyte preparation of potassium ferrocyanide ($K_4[Fe(CN)_6]$). Deionized water for rinsing and diluting all the substances was used.

Synthesis of GO powder

The modified Hummer's method was employed to synthesize GO. Initially, 23 mL of 98% concentrated sulfuric acid (H_2SO_4) was combined with 1 g of graphite

powder and 0.5 g of sodium nitrate ($NaNO_3$). The mixture was stirred at 700 rpm for 30 min in an ice bath (Yusoff, Suresh & Khairul 2022; Yusoff, Rosli & Ghadimi 2021). Gradually, 3 g of potassium permanganate ($KMnO_4$) was added, and the solution was stirred for 2 h, changing colour from black to green. After stirring at room temperature for 30 min, 46 mL of deionized water was added, and the mixture was heated to 98 °C and stirred for another 30 min (Sujiono et al. 2020). An additional 40 mL of deionized water was then added, and the mixture was stirred at 250 rpm for 15 min, turning from green to brown. To stop the reaction, 10 mL of 30% hydrogen peroxide (H_2O_2) was added, followed by stirring at 250 rpm for 15 min. To neutralise the pH and eradicate impurities, the solution was rinsed with deionized water and 5% hydrochloric acid (HCl) solution. The GO precipitate was filtered and dried at 60 °C for 12 h in an oven.

Chemical reduction of GO

450 mL of deionised water was vigorously stirred at 600 rpm after approximately 0.9 g of GO powder was added. For a duration of 30 min, the mixture was heated to 80 °C. 15 mL of 80% hydrazine hydrate was introduced into the solution after it had been thoroughly mixed. The solution was then stirred for an additional 2 h while the temperature was maintained at 80 °C. The solution was allowed to settle to room temperature after stirring. The solution was subsequently filtered and desiccated in an oven at 70 °C for 12 h.

Synthesis of rGO/Fe_3O_4/Ag Nanocomposite

The rGO/Fe_3O_4/Ag nanocomposite was fabricated using simple and low-cost method via one-pot synthesis technique. Initially, a quantity of 0.05 g of synthesized GO powder was mixed with 200 mL of deionized water and stirred for 2 h at 700 rpm. $FeCl_3 \cdot 6H_2O$ (2.02 g) and $FeCl_2 \cdot 4H_2O$ (0.74 g) were prepared in a separate beaker at a molar ratio of 2:1 by mixing with 20 mL of deionized water. The solution was then gradually added to the GO solution at ambient temperature. 1 M NaOH solution (250 mL) was prepared and added to the mixture to maintain the pH at 11. The mixture was agitated and heated for 2 h at 85 °C. Then, GO/Fe_3O_4 precipitate was extracted from the waste solvent by centrifuging and washing the mixture with deionized water after 2 h. The precipitate was then added to 150 mL of deionized water and stirred. Next, 0.079 g of $AgNO_3$ was added to the solution and stirred for 30 min at 600 rpm. Next, 2.38 g of $NaBH_4$ (98%) was introduced to the mixture, which was then agitated at 80 °C for 2 h. To eliminate any additional impurities, the solution was allowed to settle to room temperature and subsequently filtered and rinsed with ethanol. The resultant composite was further dried in an oven at 60 °C for 12 h.

Physicochemical Characterization of rGO/Fe_3O_4/Ag Nanocomposite

The rGO/Fe_3O_4/Ag nanocomposite's properties were comprehensively analysed through the use of a variety of physicochemical techniques. The functional groups in the nanocomposite were identified using Fourier Transform Infrared (FTIR) spectroscopy (Thermo Fisher Scientific, US). The composite material's external morphology was investigated using Scanning Electron Microscopy (SEM) (Tescan, Czech Republic). The nanocomposite's phase identification was ascertained through X-ray diffraction (XRD) analysis (Rigaku, Japan). Furthermore, the elemental composition of the nanocomposite was confirmed using Scanning Electron Microscopy-Energy Dispersive X-ray (SEM-EDX) (Tescan, Czech Republic). The ASAP 2020 Micrometrics instrument was employed to analyse the nanocomposite's porosity and surface area using the Brunauer-Emmett-Teller (BET) method.

Preparation of the Composite Modified-Electrode

Before conducting any electrochemical operations, the glassy carbon electrode (GCE) was polished with alumina polishing suspension that had been diluted with distilled water. After polishing, the GCE was cleaned and dried. Subsequently, 10 µL of the catalytic material was drop-casted onto the GCE. The drop-casted electrode was then left to dry at room temperature to ensure proper adhesion of the catalytic material. Once dried, the modified GCE was ready for use in electrochemical experiments, where it was immersed in an electrolyte solution for testing.

Electrochemical Activity of the Composite Modified-Electrode

Both cyclic voltammetry (CV) and linear sweep voltammetry (LSV) methods were executed using a potentiostat. In this analysis, the modified glassy carbon electrode (GCE) was employed as the working electrode, platinum as the counter electrode, and Ag/AgCl as the reference electrode. All the electrodes were sourced from Metrohm, Malaysia. Potassium ferrocyanide, $K_4[Fe(CN)_6]$, was used as the electrolyte. A 5 mmol/L solution of $K_4[Fe(CN)_6]$ was prepared by dissolving 0.412 g of $K_4[Fe(CN)_6]$ and 18.638 g of KCl in 250 mL of deionized water. The GCE was modified by depositing GO, rGO, rGO/Fe_3O_4, and rGO/Fe_3O_4/Ag via drop casting technique. The applied potential for CV ranged from -0.2 V to 0.8 V, and the optimization of scan rates for all the composites was conducted at 10, 50, 100, 150, and 200 mV/s.

ORR Analysis

The ORR analysis of the modified GCE was performed using cyclic voltammetry in a KOH solution as the electrolyte. 0.1 M KOH solution was prepared and deaerated by purging

with N_2 and O_2 gases for 10 min. The analysis was scanned five times in the potential range of -1.1 V to 0.2 V. The scanning was repeated several times to obtain consistent responses. The modified GCE was carefully monitored to ensure that no gas bubbles formed on the electrode surface, which could interfere with the measurements. Additionally, the temperature of the electrolyte solution was maintained at 25 °C to ensure the accuracy and reproducibility of the ORR analysis.

RESULTS AND DISCUSSION

Synthesis of rGO/Fe_3O_4/Ag

A modified one-pot synthesis method was used to produce rGO/Fe_3O_4/Ag nanocomposites, enabling direct synthesis in a single reaction (Hsu et al. 2024; Shen et al. 2021). GO was synthesized by adding sulfuric acid to graphite, turning the solution black. Potassium permanganate was added, changing the colour to green due to Mn_2O_7 formation. This reaction was controlled in an ice bath to prevent overheating (Sujiono et al. 2020). Deionized water was added to enhance oxidation stability, turning the solution brown. The addition of hydrogen peroxide halted the reaction, and subsequently, the mixture was flushed with HCl and deionized water. For rGO synthesis, GO was mixed with deionized water, turning the solution greenish brown. Hydrazine hydrate was added as a reducing agent, changing the colour to black for the reduction of graphene oxide (GO) to reduced graphene oxide (rGO) due to its strong reducing ability, which is essential for removing oxygen-containing groups from GO. The reaction can be represented as follows:

$$GO + N_2H_4 \rightarrow GO + H_2O$$

In the synthesis of rGO/Fe_3O_4 nanoparticles, a 2:1 molar ratio of $FeCl_3 \cdot 6H_2O$ and $FeCl_2 \cdot 4H_2O$ was used to ensure the formation of magnetite (Fe_3O_4) under alkaline conditions. The reduction of Fe (III) to Fe (II) and the subsequent precipitation of magnetite is shown in the following reaction:

$$Fe^{3+} + Fe^{2+} + 2\ OH^- \rightarrow Fe_3O_4(S)$$

The solution was then added to GO and deionized water, with ammonia used to adjust the pH to 11. Hydrazine hydrate reduced the mixture to rGO/Fe_3O_4, and the solution was rinsed with ethanol and deionized water. For rGO/Fe_3O_4/Ag synthesis, sodium hydroxide was used to maintain the pH at 11. After centrifugation to extract GO/Fe_3O_4, silver nitrate was added to introduce silver nanoparticles. Then, the $NaBH_4$ was used for the reduction of silver ions (Ag^+) to silver nanoparticles (AgNPs), with the reaction represented as follows:

$$Ag^+ + BH_4^- \rightarrow Ag\ (NP) + BH_3$$

Each of these reagents and reaction conditions was selected based on their ability to facilitate the formation of the desired nanocomposite while maintaining the required properties for ORR catalysis.

Physicochemical characterization of rGO/Fe_3O_4/Ag Nanocomposites

The Fourier Transform Infrared Spectroscopy (FTIR) technique was employed to determine the specific functional groups that are present in the synthesised nanocomposites. The FTIR spectra for GO, rGO, Fe_3O_4, rGO/Fe_3O_4, and rGO/Fe_3O_4/Ag composites are shown in Figure 1(A), with peak assignments summarized in Table 1. The detected spectral shifts and the presence or absence of specific peaks provide significant insights into the chemical interactions among the constituent materials - graphene oxide (GO), reduced graphene oxide (rGO), Fe_3O_4, and Ag nanoparticles. The extensive O–H stretching vibration at 3325.28 cm^{-1} in GO signifies a substantial presence of hydroxyl groups, commonly introduced during oxidation through the modified Hummer's method (Muhamad & Yusoff 2018; Yusoff, Suresh & Khairul 2022). The peak at 1728.22 cm^{-1} is attributed to C=O stretching in carboxyl and carbonyl functional groups resulting from the oxidative cleavage of carbon-carbon bonds. These groups are highly polar and contribute to pronounced infrared absorption due to substantial alterations in dipole moments during vibration.

The reduction of GO to rGO results in the disappearance of peaks in the 3300–3400 and 1700 cm^{-1} regions, indicating the partial removal of oxygen-containing functionalities and confirming successful deoxygenation. This reduction reinstates sp^2-hybridized carbon networks, thereby augmenting electrical conductivity. The residual C–O stretching peak at approximately 1203.58 cm^{-1} indicates incomplete reduction, suggesting the presence of residual epoxide or hydroxyl groups on the rGO surface. These residual groups can serve as anchoring or nucleation sites for nanoparticle attachment and may also engage in catalytic reactions by promoting electron transfer or the adsorption of reactants. The broad peak at approximately 501.49 cm^{-1} in Fe_3O_4 and its composites is ascribed to Fe–O lattice vibrations, indicative of the inverse spinel structure of magnetite (Fodjo et al. 2017). The amalgamation of Fe_3O_4 with rGO engenders supplementary interactions between the metal oxide and the carbon framework. The appearance of new bands at 1735.93 and 1743.64 cm^{-1} in rGO/Fe_3O_4 and rGO/Fe_3O_4/Ag indicates coordinated C=O stretching vibrations, likely attributable to carboxyl-metal bonding or interfacial charge transfer (Song et al. 2022). These alterations indicate electron reallocation at the interface, resulting in altered vibrational energies.

The distinctive peak at 1828.52 cm^{-1} in rGO/Fe_3O_4/Ag is presumably associated with C–Ag interactions or asymmetric vibrations in newly established metal-carbon-oxygen configurations. The establishment of Ag–C or Ag–O bonds can modify the local electronic milieu,

thereby affecting the dipole properties and consequently the vibrational frequency. These interactions indicate that silver nanoparticles are not solely physically adsorbed but are chemically interacting with the rGO and Fe_3O_4 matrix, potentially establishing coordination or covalent-like bonds. The peaks at 1620.21 and 1643.35 cm^{-1}, associated with C=C stretching of the conjugated sp^2 carbon framework, are prominent in rGO-containing composites, signifying the preservation of the graphene structure during composite formation. This structural retention is essential for preserving high electrical conductivity and mechanical integrity. These results also align with previous studies, confirming successful FTIR analysis of the composites.

X-ray Diffraction (XRD) was utilized to determine the average crystalline size and identify the diffraction peaks of the synthesized nanocomposites. The XRD spectra for GO, rGO, Fe_3O_4, rGO/Fe_3O_4, and rGO/Fe_3O_4/Ag composites are presented in Figure 1(B) and Table 2 shows the summary of the diffraction peaks for all the nanocomposites. From the XRD spectra, it is evident that GO exhibits a characteristic peak at $2\theta = 10.24°$, confirming its successful synthesis. Upon reduction to rGO, this peak shifts to $2\theta = 24.06°$. This deviation indicates the reduction of oxygen-containing functional groups and the restoration of C-C bonds in the composite, leading to a more ordered structure (Song et al. 2022; Yusoff, Suresh & Khairul 2022). The broadness of the peak in rGO is attributed to the presence of disordered sheets, which is typical for reduced graphene oxide (Muhamad & Yusoff 2018).

The XRD patterns for Fe_3O_4, rGO/Fe_3O_4, and rGO/Fe_3O_4/Ag show similar peaks, indicating the successful

TABLE 1. The wavenumbers (cm^{-1}) are determined based on the functional groups found in all the nanocomposites

Functional groups	Nanocomposites				
	GO	rGO	Fe_3O_4	rGO/Fe_3O_4	rGO/Fe_3O_4/Ag
O-H	3325.28	-	3363.86	3008.95	3332.99
C=O	1728.22	-	-	1735.93	1743.65
C=C	1620.21	1620.21	-	1643.35	1643.35
C-O	1172.72	1203.58	1203.58	1311.59	1203.58
C-Fe	-	-	501.49	501.49	501.49
C-Ag	-	-	-	-	1828.52

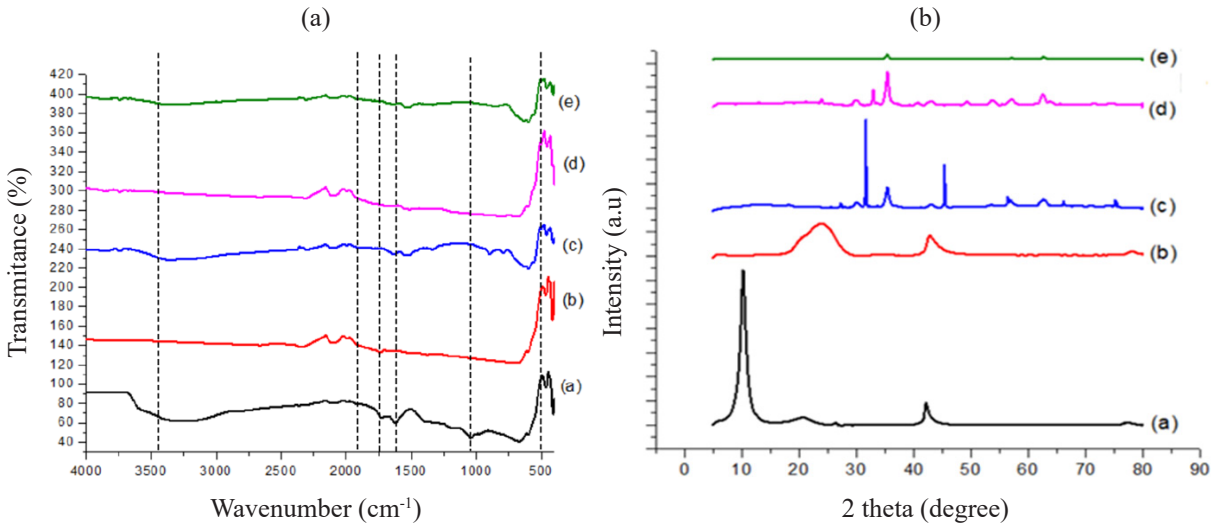

FIGURE 1. (A) FTIR for (a) GO, (b) rGO, (c) Fe_3O_4, (d) rGO/Fe_3O_4, (e) rGO/Fe_3O_4/Ag. (B) XRD spectra of (a) GO (b) rGO (c) Fe_3O_4 (d) rGO/Fe_3O_4, and (e) rGO/Fe_3O_4/Ag

incorporation of Fe_3O_4 into the composites. Peaks corresponding to the (220), (311), (400), (511), and (440) planes were observed, confirming the formation of magnetite (Fe_3O_4). The intensity and position of these peaks suggest a well-defined crystalline structure. Nevertheless, the presence of silver (Ag) nanoparticles in the composite is confirmed by an additional peak at $2\theta = 73.97°$ in the rGO/Fe_3O_4/Ag spectrum. The rGO/Fe_3O_4/Ag nanocomposite with Ag nanoparticles has been successfully synthesised, as this peak is not observable in the spectra of GO, rGO or Fe_3O_4.

Average crystallite sizes were calculated using the Scherrer equation, based on the FWHM of the primary diffraction peaks (Table 2). The sizes for rGO/Fe_3O_4 and rGO/Fe_3O_4/Ag were found to be 2.08 nm and 7.30 nm, respectively, suggesting that Ag nanoparticle incorporation increases the average crystallite size (Saha et al. 2024). Additionally, slight peak shifts and intensity variations observed in the composites suggest lattice distortion or strain due to nanoparticle integration, which may influence electronic properties and catalytic behavior. These diffraction peaks correspond well with standard JCPDS card data, confirming phase purity and composite formation.

Scanning Electron Microscopy with Energy Dispersive X-ray (SEM-EDX) was employed to observe the surface morphology and chemical elements present in the synthesized nanocomposites. The analysis was performed at a magnification of 5000X with an accelerating voltage of 15kV. The SEM images showed distinct surface morphologies for the various nanocomposites. Figure 2(a) shows that GO has a more wrinkled surface compared to rGO (Figure 2(b)), which appears smoother and more crumpled. This difference is ascribed to the reduction of hydroxyl functional groups by hydrazine hydrate during the synthesis process, leading to new C-C bonding and stacking of layers in rGO (Jaafar et al. 2018). The smoother, crumpled morphology of rGO suggests fewer defects and a more ordered structure compared to GO, which is beneficial for its application in composite materials. In Figure 2(c), Fe_3O_4 appears agglomerated, indicating a tendency of iron oxide nanoparticles to cluster together. This aggregation can detrimentally affect the material's performance by diminishing the surface area that is available. However, in the rGO/Fe_3O_4 composite, as depicted in Figure 2(d), the magnetite nanoparticles are well-dispersed across the smooth surface of rGO. The dispersion of Fe_3O_4 on rGO enhances the composite's surface area, improving its catalytic and electrochemical properties.

The SEM images showed notable agglomeration of Fe_3O_4 nanoparticles when synthesized alone, which could reduce the effective surface area and limit catalytic activity due to decreased active site availability. However, in the rGO/Fe_3O_4 and rGO/Fe_3O_4/Ag composites, the Fe_3O_4 nanoparticles showed better dispersion on the rGO sheets, likely due to the interaction between the nanoparticles and the graphene substrate. To further mitigate agglomeration, future work could explore the use of surfactants, controlled nucleation techniques, or sonication during synthesis. The SEM image of rGO/Fe_3O_4/Ag (Figure 2(e)) demonstrates that silver nanoparticles are distributed alongside iron oxide nanoparticles on the rGO surface. The homogeneous distribution of Ag and Fe_3O_4 nanoparticles on rGO suggests a strong interaction between the components, which can enhance the composite's overall conductivity and catalytic activity. The incorporation of Ag nanoparticles is particularly beneficial as it provides additional active sites for catalysis and improves the electron transfer rate within the composite.

The elemental quantification by SEM-EDX (Figure 3 & Table 3) was then conducted to confirm the elemental composition and mass percentages in the nanocomposites. The calculated mass percentages for GO indicate successful synthesis using the modified Hummer's method (Yusoff, Rosli & Ghadimi 2021). The oxygen mass percentage in rGO is fewer than in GO, validating the reduction process using hydrazine hydrate. The reduction in oxygen content confirms the successful conversion of GO to rGO, indicating the removal of oxygen-containing functional groups and the restoration of the carbon network. The elemental composition study in Table 3 shows a C/O ratio of 1.62 for graphene oxide, signifying a higher percentage of oxygenated functional groups on its surface. Upon reduction to rGO, the C/O ratio rises to 4.37, indicating a significant decrease in oxygen concentration and validating the successful transformation of GO to rGO.

TABLE 2. Diffraction peaks and average crystallite size for all the nanocomposites

Composites	Peaks	Average crystallite size, D (nm)
GO	10.24^o	9.19
rGO	24.06^o	5.01
MNP	27.31^o, 31.47^o, 43.04^o, 56.93^o, 66.16^o	8.19
rGO/MNP	22.87^o, 32.97^o, 43.09^o, 56.97^o, 62.46^o	2.08
rGO/MNP/Ag	29.98^o, 35.38^o, 43.05^o, 56.97^o, 62.67^o, 73.97^o	7.30

This reduction results in improved electrical conductivity and a more graphitic structure, advantageous for catalytic applications. Fe_3O_4 showed iron and oxygen contents of 69.88% and 30.12%, respectively, consistent with stoichiometric magnetite, the higher iron content resulting from NaOH-aided precipitation. The high iron content suggests a high loading of Fe_3O_4 in the composite, which is desirable for applications requiring magnetic properties and catalytic activity. In the rGO/Fe_3O_4 composite, the higher percentage of iron compared to carbon and oxygen confirms the incorporation of Fe_3O_4 into rGO, demonstrating successful synthesis of the hybrid material. The Ag (%) in the rGO/MNP/Ag composite is measured at 0.14%. Although silver comprises a minor portion of the composite, its inclusion is important in augmenting the electrochemical characteristics of the material, presumably boosting catalytic efficacy for processes like the oxygen reduction reaction (ORR). Despite the low concentration, the presence of silver nanoparticles is significant as it enhances the electrochemical properties of the composite (Azadmanjiri et al. 2018).

The composites were subjected to Brunauer-Emmett-Teller (BET) analysis to examine their surface area and porosity. This was done by analyzing the physical adsorption of N_2 gas into the samples at a temperature of 78 K (Baldovino-Medrano, Niño-Celis & Isaacs Giraldo 2023). Table 4 provides a summary of the surface area, pore size and pore volume. The data summarized in Table 4 indicates that GO exhibits the largest surface area (391.88 m^2/g) among the composites, followed by rGO (197.34 m^2/g), Fe_3O_4 (79.99 m^2/g), rGO/Fe_3O_4 (124.41 m^2/g), and rGO/Fe_3O_4/Ag (81.60 m^2/g). While GO maintains the highest surface area, the surface area of rGO/Fe_3O_4/Ag is significantly lower, highlighting the impact of nanoparticle deposition on the rGO structure.

The reduction in surface area, pore size, and pore volume upon the addition of Ag and Fe_3O_4 to rGO can be attributed to the non-porous nature of silver nanoparticles. Since silver does not inherently contribute to pore formation, its deposition onto rGO sheets, along with Fe_3O_4 nanoparticles, results in partial coverage of the rGO surface (Zhao et al. 2018). This coverage obstructs some of the pores, leading to a decrease in surface area and pore volume compared to the pure rGO and GO samples. However, despite the reduced surface area, the presence of these nanoparticles is not detrimental to electrochemical performance. Despite the physical BET surface area of the rGO/Fe_3O_4/Ag composite being inferior to that of GO, the distribution of Fe_3O_4 and Ag nanoparticles on the rGO sheets significantly enhances the electrochemically active surface area. This optimized active surface promotes electron transfer and increases the density of catalytic sites, resulting in higher electrochemical performance despite a diminished overall physical surface area.

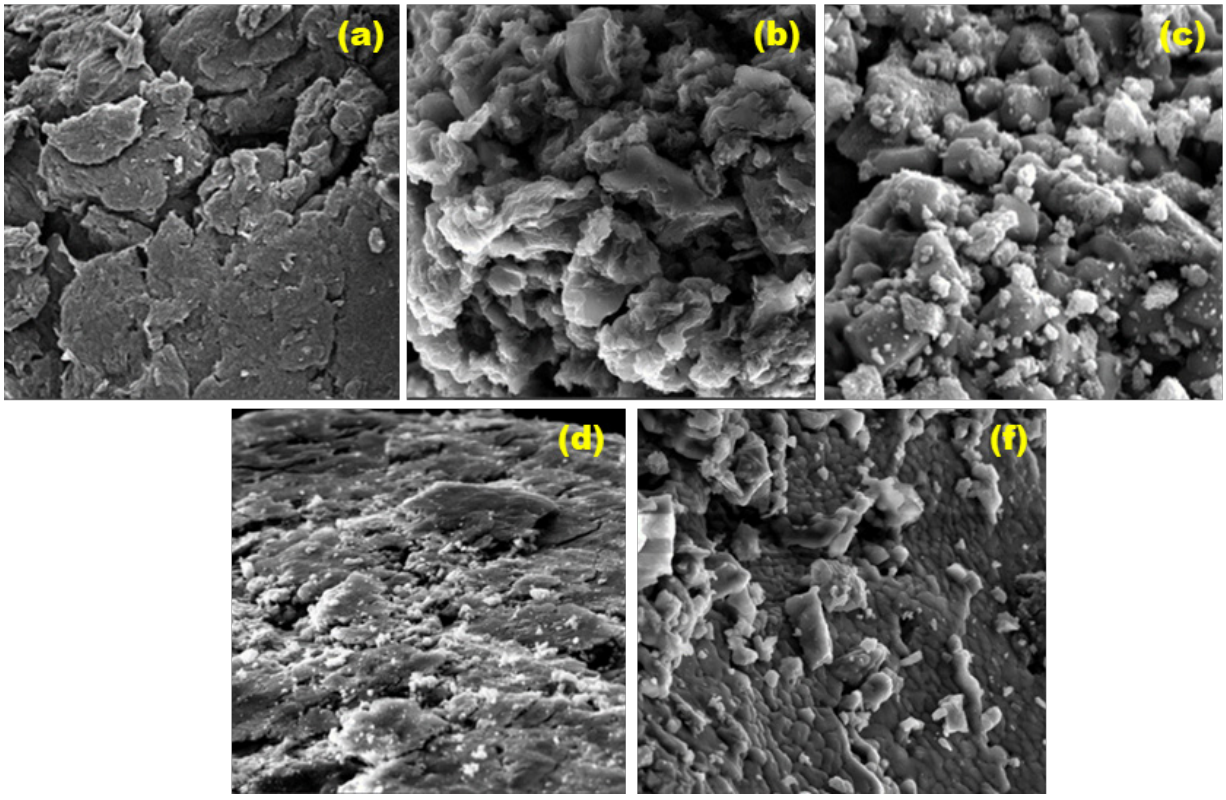

FIGURE 2. SEM images of (a) GO (B) rGO (c) Fe_3O_4 (d) rGO/Fe_3O_4, and (e) rGO/Fe_3O_4/Ag

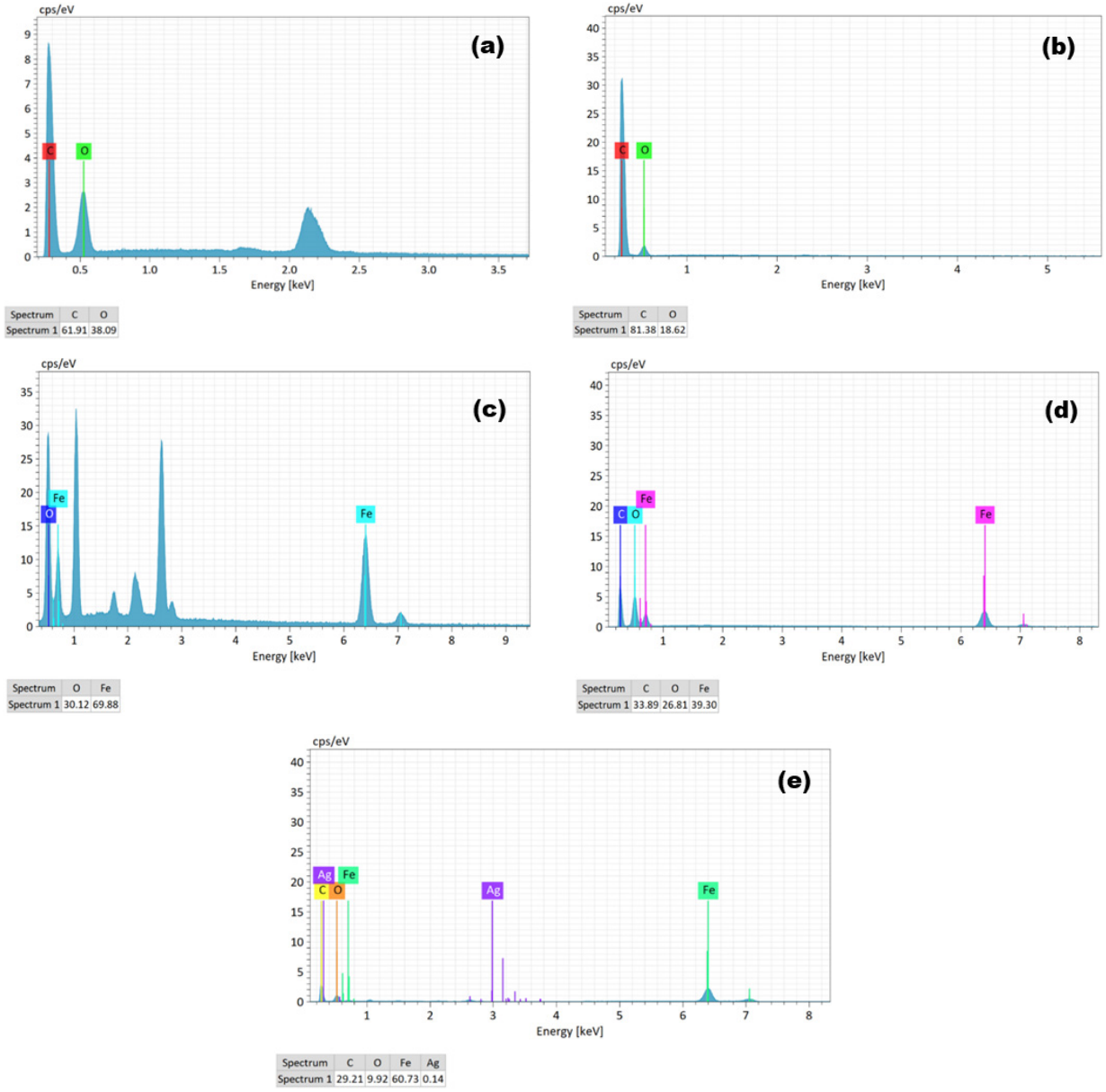

FIGURE 3. Elemental analysis of (a) GO (b) rGO (c) Fe_3O_4 (d) rGO/Fe_3O_4, and (e) rGO/Fe_3O_4/Ag

TABLE 3. Elemental composition analysis for all composites

Composites	C (%)	O (%)	Fe (%)	Ag (%)
GO	61.91	38.09	-	-
rGO	81.38	18.62	-	-
MNP	-	69.88	30.12	-
rGO/MNP	33.89	26.81	39.30	-
rGO/MNP/Ag	29.21	9.92	60.73	0.14

The observed increase in pore size in rGO/Fe_3O_4/Ag (13.43 nm) relative to rGO (6.14 nm) and rGO/Fe_3O_4 (7.78 nm) is somewhat paradoxical, considering the deposition of Ag and Fe_3O_4. The enlargement of pore size can be ascribed to structural alterations caused by the inclusion of nanoparticles. The nanoparticles obstruct certain smaller pores, potentially resulting in the development of larger mesopores or the reconfiguration of graphene layers to generate new voids, hence increasing the average pore size (Saha et al. 2024). Consequently, the reduction in surface area, anticipated due to pore obstruction by nanoparticles, is counterbalanced by the enhanced electrochemical activity resulting from the composite's altered surface architecture and superior electron transfer efficiency. The alterations in surface area and pore architecture are vital for improving the composite's electrochemical efficacy, especially in applications like the oxygen reduction reaction (ORR), where fast diffusion and efficient charge transfer are crucial.

Figure 4(a) shows nitrogen adsorption isotherm plot for GO, rGO, and rGO/Fe_3O_4/Ag. All composites exhibit type-IV isotherms, characteristic of capillary condensation occurring in mesoporous materials, where pore diameters fall in the range of 2-50 nm. This confirms that GO, rGO, and rGO/Fe_3O_4/Ag are mesoporous, making them suitable for electrochemical applications as they can enhance electron transfer rates on the electrode surface. The hysteresis loops observed in the isotherms vary among the composites, reflecting differences in pore structure. GO displays an H2(a) hysteresis loop, which is indicative of broader pore widths and ink-bottle shaped pores. In contrast, rGO, Fe_3O_4, rGO/Fe_3O_4, and rGO/Fe_3O_4/Ag exhibit H2(b) hysteresis loops, which are typical of mesopores with narrower pore widths and more uniform shapes. The shift from H2(a) in GO to H2(b) in rGO and the composites suggests that the reduction process and subsequent incorporation of Fe_3O_4 and Ag nanoparticles result in the alteration of pore structure, likely due to partial filling or reorganization of the graphene layers and the formation of new mesopores within the composites (Kumar et al. 2018; Zhao & Yuan 2021).

The BET surface area analysis corroborates these findings, showing that GO possesses the highest surface area, which decreases after reduction to rGO and further decreases upon the incorporation of Fe_3O_4 and Ag nanoparticles. This reduction in surface area is consistent with the formation of a denser composite material with smaller pore sizes and more limited accessibility to the internal surface area. Despite the decrease in surface area, the mesoporous nature of these composites remains

TABLE 4. Summary of surface area, pore size and pore volume of composites

	GO	rGO	Fe_3O_4	rGO/Fe_3O_4	rGO/Fe_3O_4/Ag
Surface area (m^2/g)	391.88	197.34	79.99	124.41	81.60
Pore size (nm)	17.34	6.14	5.21	7.78	13.43
Pore volume (cm^3/g)	1.41	0.26	0.15	0.22	0.27

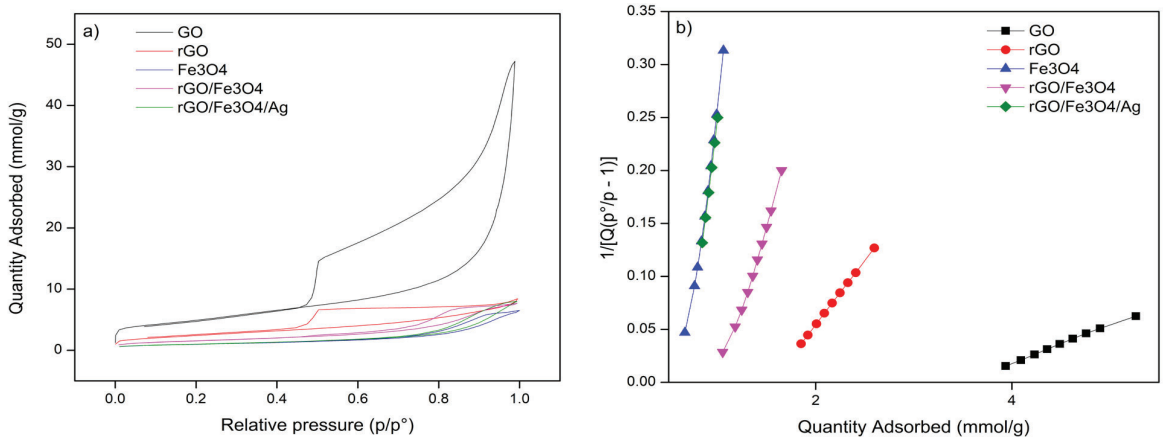

FIGURE 4. (a) Nitrogen adsorption isotherm plot of GO, rGO, Fe_3O_4, rGO/Fe_3O_4 and rGO/Fe_3O_4/Ag. (b) BET surface area plot of GO, rGO, Fe_3O_4, rGO/Fe_3O_4, and rGO/Fe_3O_4/Ag

advantageous for electrochemical applications, where controlled pore sizes and accessible active sites are critical for optimizing electron transfer and enhancing catalytic performance.

Figure 4(b) presents the corresponding BET plots, which further elucidate the textural properties of these materials. The linearity observed in the BET plots for GO and rGO indicates a relatively homogeneous pore distribution, while the non-linear segments in the plots for Fe_3O_4, rGO/Fe_3O_4, and rGO/Fe_3O_4/Ag suggest the presence of multiple pore sizes and the potential formation of micropores or smaller mesopores within these composites. The varying slopes in these plots correspond to differences in adsorption capacity, with GO exhibiting the highest quantity adsorbed, followed by rGO, Fe_3O_4, and the rGO/Fe_3O_4 composites. This trend is indicative of the influence of surface area and porosity on the adsorption properties of the materials. The presence of Fe_3O_4 in the composite contributes to the magnetic properties, which can be beneficial for applications where magnetic separation or manipulation is required. Moreover, the incorporation of Ag nanoparticles in the rGO/Fe_3O_4/Ag composite is likely to enhance the electrical conductivity and catalytic activity due to the synergistic effects of the metal nanoparticles and the graphene matrix.

Electrochemical Characterization of rGO/Fe_3O_4/Ag Nanocomposites

The electrochemical efficiency of the modified electrodes was evaluated using cyclic voltammetry (CV). The base electrode was the glassy carbon electrode (GCE), which was subsequently altered by casting nanocomposites, including GO, rGO, rGO/Fe_3O_4, and rGO/Fe_3O_4/Ag, using the drop-cast method (Accogli et al. 2021; Tipsawat et al. 2018). The CV experiments were conducted at a scan rate of 100 mV/s. The CV voltammograms, illustrated in Figure 5(a), indicate that the rGO/Fe_3O_4/Ag/GCE electrode produces significant redox responses compared to the bare GCE. The enhanced peak currents observed for rGO/Fe_3O_4/Ag suggest higher electrical conductivity and improved electrochemical activity. This enhanced performance can be ascribed to the synergistic effects of rGO, Fe_3O_4, and Ag nanoparticles, which together facilitate efficient charge transfer and improve the quantity of active sites available for redox reactions.

Cyclic voltammetry tests (Figure 5(a)) indicate that the peak current for the rGO/Fe_3O_4/Ag-modified GCE is almost 3.5 times greater than that of the unmodified GCE, demonstrating a substantial increase in electrochemical activity. This enhancement signifies enhanced electrical conductivity and an increased quantity of active sites for redox reactions, resulting from the synergistic integration of conductive rGO, catalytically active Fe_3O_4, and highly conductive Ag nanoparticles. These quantitative data strongly validate the composite's enhanced performance as an electrocatalyst. The increased peak currents reflect the high electrical conductivity and efficient charge transfer capabilities of the composite (Zhang et al. 2018). The rGO provides a high surface area and excellent conductivity, while Fe_3O_4 and Ag nanoparticles contribute additional active sites for redox reactions (Chen et al. 2021; Çıplak & Yıldız 2023).

The presence of Ag nanoparticles, known for their excellent conductivity, improves electron transfer within the composite, leading to faster reaction kinetics and higher peak currents (Darabdhara et al. 2019). The rGO/Fe_3O_4/Ag composite has a high surface area due to the dispersion of nanoparticles on the rGO sheets, increasing the number of active sites available for electrochemical responses (Zhang et al. 2019). Additionally, the drop-cast method used to deposit the nanocomposites on the GCE facilitates efficient diffusion of ions onto the electrode surface, resulting in improved interaction between the electrolyte and the electrode, enhancing the overall electrochemical efficiency. The CV curves of the rGO/Fe_3O_4/Ag/GCE at various scan rates, ranging from 50 to 250 mV/s, are shown in Figure 5(b). The slightly symmetrical redox peaks obtained at different scan rates suggest the redox processes occurring on the rGO/Fe_3O_4/Ag/GCE are reversible and controlled by diffusion. The peak current increases gradually with the square root of the scan rate as the scan rate increases, confirming that the electrochemical processes are governed by diffusion rather than surface-confined reactions. This linearity indicates efficient charge transfer within the composite, which is crucial for applications in sensors and energy storage devices where rapid and reversible electrochemical reactions are required.

Figure 5(c) further supports this conclusion by showing a plot of the peak current (I_p) versus the square root of the scan rate ($v^{1/2}$). The linear relationship, with high correlation coefficients ($R^2 > 0.99$), confirms that the redox processes are diffusion-controlled, as predicted by the Randles-Sevcik equation. The slopes of the anodic (I_{pa}) and cathodic (I_{pk}) currents provide insights into the electron transfer kinetics, with the steeper slope of the anodic peak indicating a slightly faster oxidation process. The close proximity of the anodic and cathodic peak potentials (ΔE_p) further suggests a low overpotential and efficient electron transfer within the rGO/Fe_3O_4/Ag composite.

ORR Analysis

The oxygen reduction reaction (ORR) performance of the modified electrodes was evaluated using cyclic voltammetry (CV) in 0.1 M KOH electrolyte, with O_2 gas purging to ensure an oxygen-rich environment. The cyclic voltammograms for all the modified electrodes are shown in Figure 6(a). The CV results indicate that the kinetic energy and current density increase significantly when the GCE is modified with nanocomposites such as GO, rGO, rGO/Fe_3O_4, and rGO/Fe_3O_4/Ag. This enhancement suggests that the modified electrodes are more viable and better adapted for the ORR process compared to

the bare GCE (Yusoff, Suresh & Khairul 2022). It also shows that the rGO/Fe_3O_4/Ag/GCE electrode exhibits the highest current density among all tested electrodes. The improved current density for the modified electrodes is indicative of more efficient electron transfer and higher catalytic activity. Additionally, a noticeable positive shift in the onset potential is observed for the rGO/Fe_3O_4/Ag composite compared to the other electrodes.

The positive change in the onset potential for the rGO/Fe_3O_4/Ag composite suggests a reduced overpotential necessary to commence the ORR. This change can be linked to the improved electronic characteristics of the composite materials. The interaction among rGO, Fe_3O_4, and Ag nanoparticles enhances the electronic structure of the composite, leading to a decrease in the energy barrier for oxygen adsorption and electron transfer. The high conductivity of rGO significantly amplifies this effect, enabling quicker electron transfer and reducing the necessary overpotential for the initiation of the ORR. The onset potential shift is a crucial parameter, as it reflects the ability of the electrode to facilitate ORR with minimal energy input, which is especially crucial for converting energy into applications, such as in fuel cell technology. The exceptional performance can be ascribed to the integrated impacts of rGO, Fe_3O_4, and Ag nanoparticles, which collectively offer a significant number of active sites and augment the rate of electron transfer. The high surface area of rGO supports the dispersion of Fe_3O_4 and Ag nanoparticles, facilitating greater interaction with oxygen molecules during the ORR process (Fan et al. 2021).

Figure 6(b) displays the cyclic voltammograms of the rGO/Fe_3O_4/Ag/GCE at various scan speeds, ranging from 5 to 100 mV/s. The progressive rise in current density as the scan rate increases suggests that the ORR occurring on the rGO/Fe_3O_4/Ag/GCE electrode is a reversible mechanism driven by diffusion. The enhanced performance, particularly at higher scan rates, suggests that the rGO/Fe_3O_4/Ag composite effectively promotes the 4-electron transfer mechanism, which directly reduces O_2 to H_2O, a more efficient pathway in ORR. The 4-electron transfer mechanism in the oxygen reduction reaction (ORR) is preferred in fuel cells due to its ability to directly convert O_2 to H_2O. This process is more efficient and generates higher current densities than the 2-electron transfer

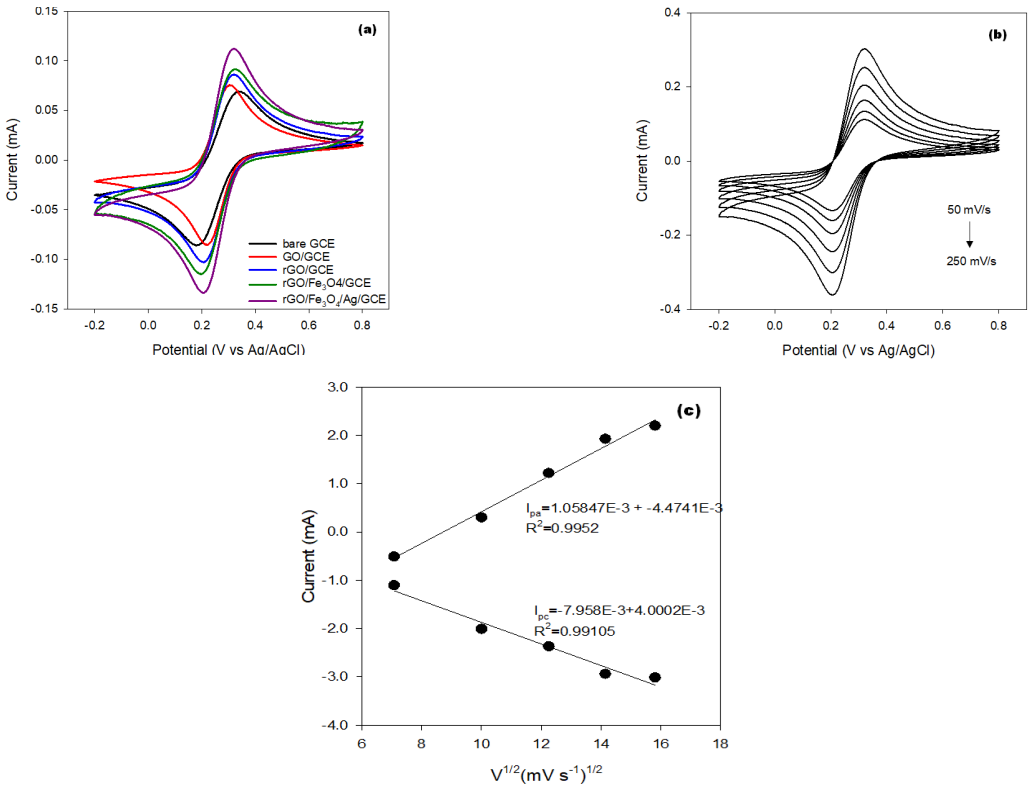

FIGURE 5. (a) Cyclic voltammograms of bare GCE, GO/GCE, rGO/GCE, rGO/Fe_3O_4/GCE, and rGO/Fe_3O_4/Ag/GCE at a scan rate of 100 mV/s, (b) Cyclic voltammograms of rGO/Fe_3O_4/Ag/GCE at different scan rates ranging from 50 to 250 mV/s, (c) Plot of peak current (I_p) vs. square root of scan rate ($v^{1/2}$) for rGO/Fe_3O_4/Ag/GCE. 5.0 mM $K_4[Fe(CN)_6]$ of 1.0 M KCl is the electrolyte used in the analysis

pathway, which results in the formation of hydrogen peroxide (H_2O_2). The rGO/Fe_3O_4/Ag composite enhances this mechanism through the synergistic interactions among its components. Reduced graphene oxide establishes a conductive framework that enhances electron transfer, whereas iron oxide presents active sites for oxygen adsorption, and silver nanoparticles boost the rates of electron transfer. The relationship between rGO and Fe_3O_4 improves the adsorption of oxygen molecules. This, in conjunction with Ag's catalytic properties, facilitates the direct reduction of O_2 to H_2O through the 4-electron pathway. Figure 6(c) compares the CV curves for the rGO/Fe_3O_4/Ag/GCE under N_2 and O_2 purging conditions. The significant increase in current density under O_2 purging highlights the efficient oxygen reduction capability of the rGO/Fe_3O_4/Ag composite. The difference in current density between N_2 and O_2 purging further confirms the active role of the composite in facilitating the ORR.

The magnetic properties of Fe_3O_4 nanoparticles are essential for boosting the activity of the oxygen reduction reaction (ORR) by promoting the binding of oxygen molecules to the surface of the electrode. This, in turn, enhances the rate at which electrons are transferred. Additionally, the presence of Ag nanoparticles, known for their excellent catalytic properties, further boosts the ORR performance by increasing the availability of active sites and accelerating the reduction process. The combination of these materials results in a composite that not only supports efficient charge transfer but also maximizes the utilization of the 4-electron reduction pathway, leading to the highest current densities observed in the study (Huang et al. 2019; Jiang et al. 2021). The overall ORR analysis confirms the successful alteration of the electrodes with the nanocomposites, with the rGO/Fe_3O_4/Ag composite showing the most promising results. The combination of rGO high surface area and conductivity, Fe_3O_4 magnetic properties and active sites, and Ag catalytic enhancement makes the rGO/Fe_3O_4/Ag composite the most effective electrode for ORR among those tested. While rGO/Fe_3O_4/Ag composites shown enhanced performance relative to bare GCE, it is essential to compare this with proven catalysts such as Pt/C. Platinum catalysts typically exhibit onset potentials around 0.95 V (vs. RHE) and current densities surpassing 5 mA/cm^2 under identical alkaline

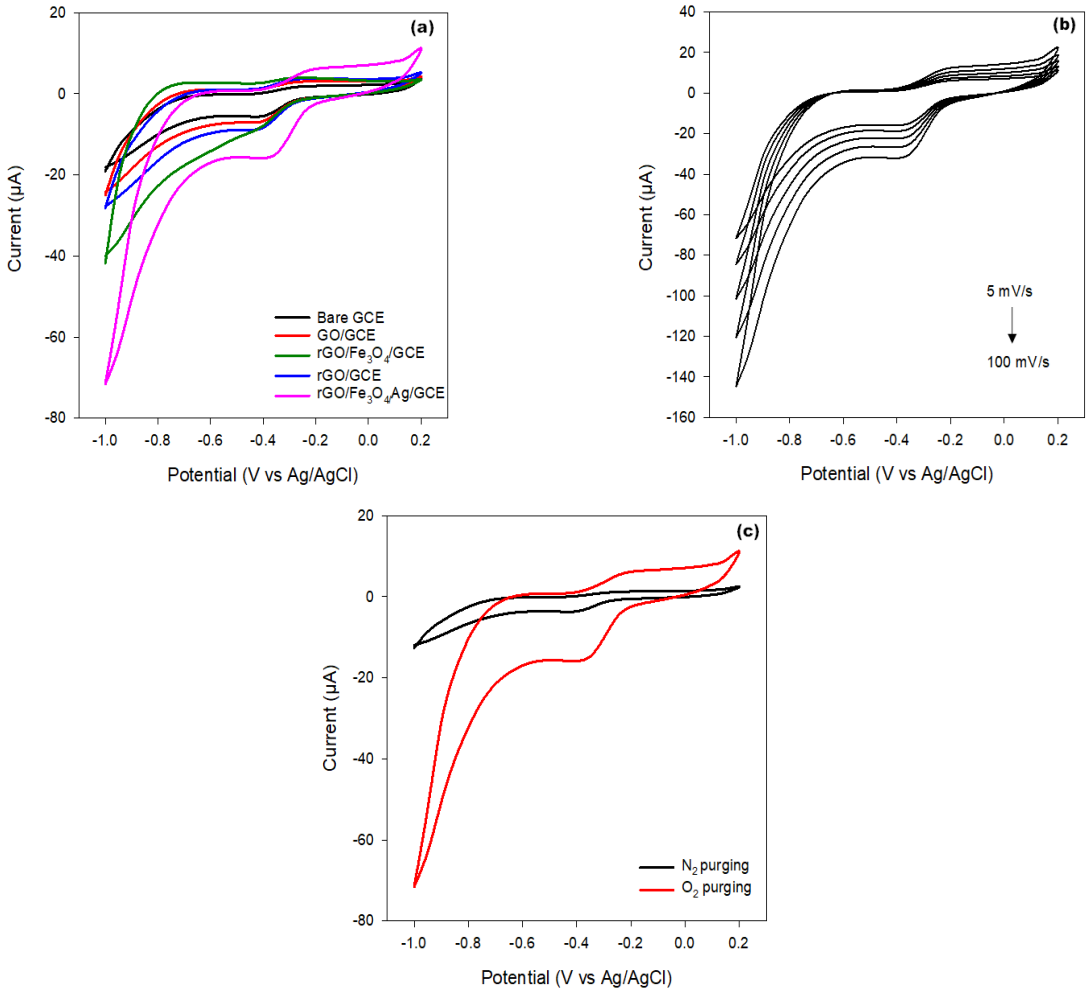

FIGURE 6. ORR analysis of modified composite electrode

circumstances (Shao et al. 2018). Conversely, the rGO/Fe_3O_4/Ag catalyst exhibited a marginally reduced onset potential and peak current density, however, remains promising. The drawback involves the substantial expense and limited availability of Pt, whereas rGO/Fe_3O_4/Ag presents a more sustainable option with satisfactory performance and remarkable stability over repeated cycling, but it still allows for additional optimisation. The high current densities and efficient electron transfer observed with this composite indicate its strong potential for utilisation in fuel cells along with other electrochemical devices that require oxygen reduction.

CONCLUSIONS

This study successfully synthesized and characterized reduced graphene oxide incorporated with iron (III) oxide and silver nanoparticles (rGO/Fe_3O_4/Ag) using a modified one-pot process. As the first investigation to employ rGO/Fe_3O_4/Ag as an ORR catalyst, the findings highlight the ability of the material to serve as a practical alternative to platinum in cathode materials. Physicochemical characterizations, including FTIR, XRD, SEM-EDX, and BET, confirmed the formation and structural integrity of the nanocomposites, with a surface area of 81.60 m^2/g. Electrochemical characterization showed that the modified rGO/Fe_3O_4/Ag exhibited significant redox responses, indicating enhanced electrochemical activity compared to the bare GCE. In the ORR analysis, the rGO/Fe_3O_4/Ag demonstrated a positive shift in the cyclic voltammogram, suggesting improved current density and superior ORR performance relative to the bare GCE. These findings strongly suggest that rGO/Fe_3O_4/Ag can be an effective replacement for platinum in ORR applications as a cathode material, offering a promising alternative for fuel cells and other electrochemical devices. Further optimization is recommended to fully harness their potential in practical application.

ACKNOWLEDGMENTS

We would like to express our gratitude to the Ministry of Higher Education, Malaysia for providing financing through the Fundamental Research Grant Scheme (FRGS/1/2021/STG04/UMT/02/1). We also appreciate the Central Lab, Universiti Malaysia Terengganu for supplying us with research facilities.

REFERENCES

Accogli, A., Bertoli, L., Panzeri, G., Gibertini, E., Pesce, R., Bussetti, G. & Magagnin, L. 2021. Electrochemical characterization of magnetite (Fe_3O_4) nanoaggregates in acidic and alkaline solutions. *ACS Omega* 6(41): 26880-26887.

Ajinkya, N., Yu, X., Kaithal, P., Luo, H., Somani, P. & Ramakrishna, S. 2020. Magnetic iron oxide nanoparticle (IONP) synthesis to applications: Present and future. *Materials* 13(20): 4644.

Azadmanjiri, J., Srivastava, V.K., Kumar, P., Wang, J. & Yu, A. 2018. Graphene-supported 2D transition metal oxide heterostructures. *Journal of Materials Chemistry A* 6(28): 13509-13537. https://doi.org/10.1039/c8ta03404d

Baldovino-Medrano, V.G., Niño-Celis, V. & Isaacs Giraldo, R. 2023. Systematic analysis of the nitrogen adsorption–desorption isotherms recorded for a series of materials based on microporous–mesoporous amorphous aluminosilicates using classical methods. *Journal of Chemical & Engineering Data* 68(9): 2512-2528.

Chandrasekaran, S., Ma, D., Ge, Y., Deng, L., Bowen, C., Roscow, J., Zhang, Y., Lin, Z., Misra, R.D.K. & Li, J. 2020. Electronic structure engineering on two-dimensional (2D) electrocatalytic materials for oxygen reduction, oxygen evolution, and hydrogen evolution reactions. *Nano Energy* 77: 105080.

Chen, T., Geng, Y., Wan, H., Xu, Y., Zhou, Y., Kong, X., Wang, J., Qi, Y., Yao, B. & Gao, Z. 2021. Facile preparation of Fe_3O_4/Ag/RGO reusable ternary nanocomposite and its versatile application as catalyst and antibacterial agent. *Journal of Alloys and Compounds* 876: 160153.

Çıplak, Z. & Yıldız, N. 2023. Ag@ Fe_3O_4 nanoparticles decorated NrGO nanocomposite for supercapacitor application. *Journal of Alloys and Compounds* 941: 169024.

Cui, C., Du, G., Zhang, K., An, T., Li, B., Liu, X. & Liu, Z. 2020. Co_3O_4 nanoparticles anchored in MnO_2 nanorods as efficient oxygen reduction reaction catalyst for metal-air batteries. *Journal of Alloys and Compounds* 814: 152239. https://doi.org/https://doi.org/10.1016/j.jallcom.2019.152239

Cui, X., Gao, L., Yang, Y. & Lin, Z. 2022. Heteroatom-doped graphene-based electrocatalysts for ORR, OER, and HER. In *Micro and Nano Technologies: Nanomaterials for Electrocatalysis*, edited by Maiyalagan, T., Khandelwal, M., Kumar, A., Nguyen, T.A. & Yasin, G. Elsevier. pp. 145-168.

Darabdhara, G., Das, M.R., Singh, S.P., Rengan, A.K., Szunerits, S. & Boukherroub, R. 2019. Ag and Au nanoparticles/reduced graphene oxide composite materials: Synthesis and application in diagnostics and therapeutics. *Advances in Colloid and Interface Science* 271: 101991.

Fan, J., Chen, M., Zhao, Z., Zhang, Z., Ye, S., Xu, S., Wang, H. & Li, H. 2021. Bridging the gap between highly active oxygen reduction reaction catalysts and effective catalyst layers for proton exchange membrane fuel cells. *Nature Energy* 6(5): 475-486.

Fodjo, E.K., Gabriel, K.M., Serge, B.Y., Li, D., Kong, C. & Trokourey, A. 2017. Selective synthesis of Fe_3O_4AuxAgynanomaterials and their potential applications in catalysis and nanomedicine. *Chemistry Central Journal* 11(1): 58. https://doi.org/10.1186/s13065-017-0288-y

Ganapathe, L.S., Mohamed, M.A., Mohamad Yunus, R. & Berhanuddin, D.D. 2020. Magnetite (Fe_3O_4) nanoparticles in biomedical application: From synthesis to surface functionalisation. *Magnetochemistry* 6(4): 68.

Goyal, D., Dang, R.K., Goyal, T., Saxena, K.K., Mohammed, K.A. & Dixit, S. 2022. Graphene: A path-breaking discovery for energy storage and sustainability. *Materials* 15(18): 6241.

Gu, W., Xu, J., Sun, J. & Zhao, T. 2023. A durable and robust Fe–N–C electrocatalyst for oxygen reduction reactions by introducing Ti_3C_2–TiO_2 as radical scavengers. *International Journal of Hydrogen Energy* 48(13): 5323-5332. https://doi.org/https://doi.org/10.1016/j.ijhydene.2022.11.048

He, X., Long, X., Wang, P., Wu, H., Han, P., Tang, Y., Li, K., Ma, X. & Zhang, Y. 2021. Interconnected 3D Fe_3O_4/rGO as highly durable electrocatalyst for oxygen reduction reaction. *Journal of Alloys and Compounds* 855: 157422.

He, Y., Liu, S., Priest, C., Shi, Q. & Wu, G. 2020. Atomically dispersed metal–nitrogen–carbon catalysts for fuel cells: Advances in catalyst design, electrode performance, and durability improvement. *Chemical Society Reviews* 49(11): 3484-3524.

Hsu, C-Y., Ali, E., Al-Saedi, H.F.S., Mohammed, A.Q., Mustafa, N.K., Talib, M.B., Radi, U.K., Ramadan, M.F., Ami, A.A. & Al-Shuwaili, S.J. 2024. A chemometric approach based on response surface methodology for optimization of antibiotic and organic dyes removal from water samples. *BMC Chemistry* 18(1): 5.

Huang, M., Liu, S., Gong, S., Xu, P., Yang, K., Chen, S., Wang, C. & Chen, Q. 2019. Silver nanoparticles encapsulated in an N-doped porous carbon matrix as high-active catalysts toward oxygen reduction reaction via electron transfer to outer graphene shells. *ACS Sustainable Chemistry & Engineering* 7(19): 16511-16519.

Idris, A. M., Shinger, M. I., Barkaoui, S., Khan, K., Idris Abdu, H., Edris, M. M., & Lu, X. 2018. Fabrication of rGO-Fe3O4 Hybrid Functionalized with Ag3PO4 as photocatalyst for degradation of Rhodamime B under visible light irradiation. *Materials Research Bulletin* 102: 100–107.

International Renewable Energy Agency. 2023. *Renewables are the Solution to Malaysia's Sustainable Future and Renewed Climate Ambition*. https://www.irena.org/News/pressreleases/2023/Mar/Renewables-Are-the-Solution-to-Malaysias-Sustainable-Future-and-Renewed-Climate-Ambition

Iriarte-Mesa, C., López, Y.C., Matos-Peralta, Y., de la Vega-Hernández, K. & Antuch, M. 2020. Gold, silver and iron oxide nanoparticles: Synthesis and bionanoconjugation strategies aiming to electrochemical applications. *Surface-Modified Nanobiomaterials for Electrochemical and Biomedicine Applications* 378(12): 93-132.

Jaafar, E., Kashif, M., Sahari, S.K. & Ngaini, Z. 2018. Study on morphological, optical and electrical properties of graphene oxide (GO) and reduced graphene oxide (rGO). *Materials Science Forum* 917: 112-116.

Jiang, P.Y., Xiao, Z.H., Wang, Y.F., Li, N. & Liu, Z.Q. 2021. Enhanced performance of microbial fuel cells using Ag nanoparticles modified Co, N co-doped carbon nanosheets as bifunctional cathode catalyst. *Bioelectrochemistry* 138: 107717.

Khan, K., Tareen, A.K., Aslam, M., Zhang, Y., Wang, R., Ouyang, Z., Gou, Z. & Zhang, H. 2019. Recent advances in two-dimensional materials and their nanocomposites in sustainable energy conversion applications. *Nanoscale* 11(45): 21622-21678.

Kumar, K., Gairola, P., Lions, M., Ranjbar-Sahraie, N., Mermoux, M., Dubau, L., Zitolo, A., Jaouen, F. & Maillard, F. 2018. Physical and chemical considerations for improving catalytic activity and stability of non-precious-metal oxygen reduction reaction catalysts. *ACS Catalysis* 8(12): 11264-11276.

Kumar, V., Gupta, R.K., Gundampati, R.K., Singh, D.K., Mohan, S., Hasan, S.H. & Malviya, M. 2018. Enhanced electron transfer mediated detection of hydrogen peroxide using a silver nanoparticle–reduced graphene oxide–polyaniline fabricated electrochemical sensor. *RSC Advances* 8(2): 619-631.

Mohammed, H., Al-Othman, A., Nancarrow, P., Tawalbeh, M. & Assad, M.E.H. 2019. Direct hydrocarbon fuel cells: A promising technology for improving energy efficiency. *Energy* 172: 207-219.

Muhamad, N.B. & Yusoff, F. 2018. The physical and electrochemical characteristic of gold nanoparticles supported pedot/graphene composite as potential cathode material in fuel cells. *Malaysian Journal of Analytical Sciences* 22(6): 921-930.

Peng, L. & Wei, Z. 2020. Catalyst engineering for electrochemical energy conversion from water to water: Water electrolysis and the hydrogen fuel cell. *Engineering* 6(6): 653-679.

Saha, S., Routray, K.L., Hota, P., Dash, B., Yoshimura, S., Ratha, S. & Nayak, T.K. 2024. Structural, magnetic and dielectric properties of green synthesized Ag doped $NiFe_2O_4$ spinel ferrite. *Journal of Molecular Structure* 1302: 137409.

Shao, Q., Li, F., Chen, Y. & Huang, X. 2018. The advanced designs of high-performance platinum-based electrocatalysts: Recent progresses and challenges. *Advanced Materials Interfaces* 5(16): 1800486.

Shao, Y., Yin, G. & Gao, Y. 2007. Understanding and approaches for the durability issues of Pt-based catalysts for PEM fuel cell. *Journal of Power Sources* 171(2): 558-566. https://doi.org/https://doi.org/10.1016/j.jpowsour.2007.07.004

Sharma, R.K., Yadav, S., Dutta, S., Kale, H.B., Warkad, I.R., Zbořil, R., Varma, R.S. & Gawande, M.B. 2021. Silver nanomaterials: Synthesis and (electro/photo) catalytic applications. *Chemical Society Reviews* 50(20): 11293-11380.

Shen, Y., Wang, Y., Fang, S., Park, J.K., Pan, C., Chen, Y., Zhu, N. & Wu, H. 2021. Novel magnetically separable Ag@ AgCl-Fe_3O_4/RGO nanocomposites for enhanced dielectric barrier discharge plasma reaction for high-performance water decontamination. *Desalination and Water Treatment* 223: 335-349.

Singh, S.K., Takeyasu, K. & Nakamura, J. 2019. Active sites and mechanism of oxygen reduction reaction electrocatalysis on nitrogen-doped carbon materials. *Advanced Materials* 31(13): 1804297.

Smith, A.T., LaChance, A.M., Zeng, S., Liu, B. & Sun, L. 2019. Synthesis, properties, and applications of graphene oxide/reduced graphene oxide and their nanocomposites. *Nano Materials Science* 1(1): 31-47.

Song, K., Wei, J., Dong, W., Zou, Z. & Wang, J. 2022. Fe_3O_4/N-CNTs derived from hypercrosslinked carbon nanotube as efficient catalyst for ORR in both acid and alkaline electrolytes. *International Journal of Hydrogen Energy* 47(47): 20529-20539.

Sujiono, E.H., Zabrian, D., Dahlan, M.Y., Amin, B.D. & Agus, J. 2020. Graphene oxide based coconut shell waste: Synthesis by modified Hummers method and characterization. *Heliyon* 6(8): e04568.

Tarcan, R., Todor-Boer, O., Petrovai, I., Leordean, C., Astilean, S. & Botiz, I. 2020. Reduced graphene oxide today. *Journal of Materials Chemistry C* 8(4): 1198-1224.

Tipsawat, P., Wongpratat, U., Phumying, S., Chanlek, N., Chokprasombat, K. & Maensiri, S. 2018. Magnetite (Fe_3O_4) nanoparticles: Synthesis, characterization and electrochemical properties. *Applied Surface Science* 446: 287-292.

Yusoff, F., Suresh, K. & Khairul, W.M. 2022. Synthesis and characterization of reduced graphene oxide/iron oxide/silicon dioxide (rGO/Fe_3O_4/SiO_2) nanocomposite as a potential cathode catalyst. *Journal of Physics and Chemistry of Solids* 163: 110551.

Yusoff, F., Rosli, A.R. & Ghadimi, H. 2021. Synthesis and characterisation of gold nanoparticles/poly3,4-ethylene-dioxythiophene/reduced-graphene oxide for electrochemical detection of dopamine. *Journal of the Electrochemical Society* 168(2): 26509.

Zhang, D., Liu, T., Cheng, J., Cao, Q., Zheng, G., Liang, S., Wang, H. & Cao, M-S. 2019. Lightweight and high-performance microwave absorber based on 2D WS_2–RGO heterostructures. *Nano-Micro Letters* 11(1): 38.

Zhang, H., Zhang, G., Tang, M., Zhou, L., Li, J., Fan, X., Shi, X. & Qin, J. 2018. Synergistic effect of carbon nanotube and graphene nanoplates on the mechanical, electrical and electromagnetic interference shielding properties of polymer composites and polymer composite foams. *Chemical Engineering Journal* 353: 381-393.

Zhao, H. & Yuan, Z.Y. 2021. Surface/interface engineering of high-efficiency noble metal-free electrocatalysts for energy-related electrochemical reactions. *Journal of Energy Chemistry* 54: 89-104.

Zhao, S., Jiang, H., Li, J., Meng, X., Chao, T., Zhang, Z., Zhang, P., Gao, Y., & Cao, D. 2018. Amorphizing of Ag Nanoparticles under Bioinspired One-step Assembly of Fe3O4-Ag/rGO Hybrids via Self-redox Process with Enhanced Activity. *Applied Organometallic Chemistry* 32(8): e4428.

Zhou, Y., Chen, G., Wang, Q., Wang, D., Tao, X., Zhang, T., Feng, X. & Müllen, K. 2021. Fe-N-C Electrocatalysts with Densely Accessible Fe-N4 Sites for Efficient Oxygen Reduction Reaction. *Advanced Functional Materials* 31(34): 2102420.

*Corresponding author; email: farhanini@umt.edu.my